REGULAR PAPER

ACTA PHYSIOLOGICA

# Intestinal mesenchymal cells regulate immune responses and promote epithelial regeneration in vitro and in dextran sulfate sodium-induced experimental colitis in mice

Laura Hidalgo-Garcia[1,2]    |    José Alberto Molina-Tijeras[1,2]    |    Francisco Huertas-Peña[2,3]    |
Antonio Jesús Ruiz-Malagón[1,2]    |    Patricia Diez-Echave[1,2]    |    Teresa Vezza[1,2]    |
María Jesús Rodríguez-Sojo[1,2]    |    Rocío Morón[2,4]    |    Patricia Becerra-Massare[5]    |
Alba Rodríguez-Nogales[1,2,6] (iD)    |    Julio Gálvez[1,2,7]    |    María Elena Rodríguez-Cabezas[1,2]    |
Per Anderson[2,8]

[1]Department of Pharmacology, Center for Biomedical Research (CIBM), University of Granada, Granada, Spain

[2]Instituto de Investigación Biosanitaria de Granada (ibs.GRANADA), Granada, Spain

[3]Servicio de Cirugía, Hospital Universitario Virgen de las Nieves, Granada, Spain

[4]Servicio Farmacia Hospitalaria, Hospital Universitario Clínico San Cecilio, Granada, Spain

[5]Servicio de Anatomía Patológica, Hospital Universitario Clínico San Cecilio, Granada, Spain

[6]Servicio de Digestivo, Hospital Universitario Virgen de las Nieves, Granada, Spain

[7]Centre for Biomedical Research in Liver and Digestive Diseases Network (CIBER-EHD), University of Granada, Granada, Spain

[8]Servicio de Análisis Clínicos e Inmunología, Hospital Universitario Virgen de las Nieves, Granada, Spain

**Correspondence**
Alba Rodríguez-Nogales and Julio Gálvez, Department of Pharmacology, Center for Biomedical Research (CIBM), University of Granada, 18071 Granada, Spain.
Email: albarn@ugr.es; jgalvez@ugr.es

**Funding information**
This work was funded by the Junta de Andalucía (CTS 164) and by the Instituto de Salud Carlos III (Spain) and Fondo Europeo de Desarrollo Regional (FEDER), from the European Union, through the research grants PI18/00826, PI0206-2016 and PI19/01058. L.H-G and A.J.R-M are predoctoral fellows funded by the Spanish Ministry of Science and Innovation ("Programa de Doctorado: Medicina Clínica y Salud Pública" B12.56.1). J.A.M-T is a predoctoral fellow from the Instituto de Salud Carlos III (FI17/00176). P.A is supported by the Consejería de Salud, Junta

**Abstract**

**Aim:** Disruption of the intestinal mucosal tolerance, that is, the immunological unresponsiveness to innocuous food antigens and the commensal microbiota, in the colon is associated with several chronic diseases including inflammatory bowel disease (IBD). Understanding the mechanisms responsible for intestinal mucosal tolerance has potential translational value for its therapy and management. Human intestinal mesenchymal cells (iMCs) play important roles in colonic mucosal tolerance, but further studies on their tissue regenerative and immunomodulatory capacities are necessary in order to fully understand their function in health and disease.

**Methods:** In this study, we have isolated and analysed the capacity of human iMCs to promote wound healing and modulate immune responses in vitro and in vivo, using the dextran sulfate sodium (DSS)-induced colitis model.

**Results:** Cultured iMCs were CD45⁻CD73⁺CD90⁺CD105⁺ and accelerated the wound closure in a normal colon mucosa (NCM) 356 human epithelial cell wound healing assay. Furthermore, iMCs blocked the LPS-mediated induction of TNF-α in

Laura Hidalgo-Garcia and José Alberto Molina-Tijeras contributed equally to the study.

María Elena Rodríguez-Cabezas and Per Anderson contributed equally to the supervision of the study.

THP-1 macrophages and inhibited the proliferation of peripheral blood mononuclear cells, partly through the induction of indoleamine-2,3-dioxygenase. In DSS colitic mice, iMCs administration reduced the disease activity index and ameliorated intestinal tissue damage and permeability. Furthermore, iMCs reduced intestinal inflammation, evidenced by a decreased mRNA expression of pro-inflammatory cytokines, reduced IL-1β secretion by intestinal explants and inhibited colonic iNOS protein expression.

**Conclusions:** Our data show that human iMCs isolated from the noninflamed intestine possess tissue-regenerative and immunomodulatory capacities that could potentially be harnessed/restored in order to reduce IBD severity.

**KEYWORDS**

dextran sulfate sodium colitis, immunomodulation, inflammatory bowel disease, intestinal mesenchymal cells, wound healing

## 1 | INTRODUCTION

Inflammatory bowel disease (IBD) is a chronic idiopathic disease mainly represented by two major forms, ulcerative colitis (UC) and Crohn's disease (CD). Although its etiology remains unknown, IBD is thought to stem from a combination of environmental factors, genetic predisposition, microbiota imbalance, and mucosa immune defects.[1] Both conditions are thought to start after a breach of the intestinal epithelial barrier, leading to excessive and sustained cytokine production and immune cell recruitment and activation.[2]

Mesenchymal stromal cells (MSCs) are nonhematopoietic, nonepithelial, nonendothelial, multipotent cells with self-renewal capacity present in almost all tissues and organs.[3] In the last decade, mounting evidence has shown that they possess the ability to repair damaged and inflamed tissues and although not considered "professional" immune cells, they can regulate immune responses through direct contact or by secreting soluble mediators.[4-7] Intestinal mesenchymal cells (iMCs) represent a heterogeneous cell population which includes MSCs, fibroblasts, myofibroblasts and pericytes. These cells reside in the subepithelial compartment where they provide much of the structural framework of the intestine. Importantly, iMCs regulate the homeostasis/maintenance of the epithelial barrier[8,9] and promote immunological tolerance against the commensal bacteria and food antigens through the expression of immunomodulatory molecules, including programmed death-ligand-1 (PD-L1),[10] chemokines and retinoic acid.[11]

However, recent studies have suggested that iMCs play important roles in both inhibiting and promoting intestinal inflammation and damage in IBD. Using a murine model of acute dextran sulfate sodium (DSS) colitis, Scheibe et al[12] showed that IL-36-receptor signaling in iMCs promoted the mucosal healing in vivo. In contrast, recent studies using single-cell RNA sequencing have identified a subset of pro-inflammatory iMCs which increase drastically in the inflamed intestine of both pediatric and adult UC patients.[13,14] This remodeling of the colonic mesenchyme in IBD patients is thought to perpetuate the intestinal inflammation and prevent the repair of the intestinal barrier.

Due to their important homeostatic function in the healthy intestine and their ambiguous role in intestinal inflammation during IBD, further analysis of their capacity to promote epithelial repair and regulate immune/inflammatory responses is of great importance when designing new therapies for intestinal inflammatory diseases. In the present study we have isolated iMCs from human colonic biopsies and demonstrate their ability to promote wound healing and regulate immune responses in vitro and in vivo, using a model of DSS-induced colitis. Our data show that human iMCs isolated from noninflamed intestine possess tissue-regenerative and immunomodulatory capacities that could potentially be potentiated/restored in order to reduce IBD disease severity.

## 2 | RESULTS

### 2.1 | Cultured iMCs show a fibroblast-like morphology and express CD73, CD90, CD105 and PD-L1

iMCs isolated from intestinal resections presented a fibroblast-like shape upon in vitro culture (Figure 1A) and lacked hematopoietic (CD45), epithelial (CD31, EpCam) and endothelial (CD34) markers, while expressing PD-L1 (CD274), CD73 (ecto-5′-nucleotidase), CD90 (thymocyte differentiation antigen 1) and CD105 (endoglin, a surface membrane glycoprotein part of the TGF-β receptor complex) (Figure 1B). These last markers are also expressed by MSCs and are transmitted to their mesenchymal lineage descendants, such as muscle cells and fibroblast.[15] This phenotype
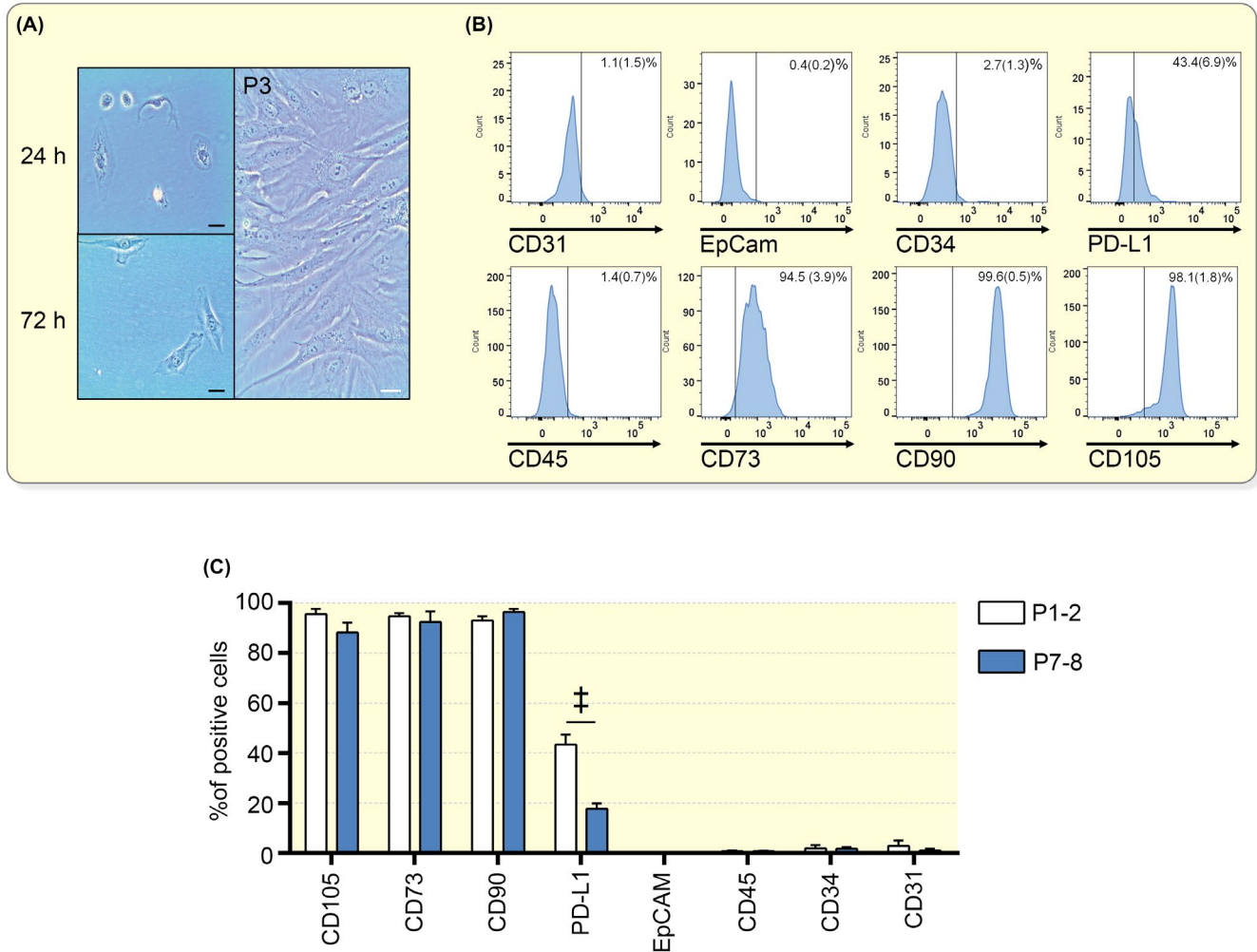
**FIGURE 1** Phenotypic characterization of human iMCs. (A) Morphology of iMCs, 24 and 72 h after isolation through plastic adherence (black lines represent 50 μm). At passage 3 (P3), the cultures consisted of homogeneously larger fibroblastic cells (white line represent 20 μm). (B) P2-3 iMCs were stained for epithelial (EpCam, CD31), endothelial (CD34), hematopoietic (CD45), mesenchymal (CD73, CD90, CD105) markers, and the immunomodulatory marker PD-L1 (CD274) and analyzed by flow cytometry. Representative histograms demonstrate specific staining and the vertical lines represent the background staining using the corresponding isotype controls. (C) Average expression levels (% of positive cells in relation to isotype control staining) of the above mentioned markers on iMCs at P1-2 and P7-8 isolated from 6 donors. Data are shown as mean (SEM). $^{‡}P < .001$

was stable across serial cell passages (from P1-2 to P7-8), being PD-L1 the only cell marker that was significantly decreased at a later passage (Figure 1C).

## 2.2 | iMCs inhibit T cell proliferation, partly through IDO

We first aimed to study the immunomodulatory characteristics of iMCs, beginning with analysing their effect on T cell proliferation. MSCs need to be "licensed" by IFN-γ and inflammatory cytokines, including TNF-α, to acquire suppressive capacities.[16,17] Thus, we co-cultured different concentrations of nonstimulated and TNF-α/IFN-γ-prestimulated iMCs with carboxyfluorescein succinimidyl ester (CFSE)-labeled peripheral blood mononuclear cells (PBMCs) in the presence of the T cell mitogen phytohemagglutinin-L

(PHA-L) (Figure 2A). In the PHA-L-stimulated cultures, the iMCs significantly inhibited the proliferation of CD4$^{+}$ and CD8$^{+}$ T cells at the highest cell concentration (20000 iMCs) (Figure 2B,C). Cytokine-primed iMCs had a significantly increased capacity to inhibit the proliferation of CD4$^{+}$ T cells, with a similar trend seen for the suppression of CD8$^{+}$ T cells (Figure 2B,C). Indoleamine-2,3-dioxygenase (IDO), prostaglandin E$_2$ (PGE$_2$) and IL-10 have been implicated in the immunomodulatory capacity of MSCs.[18] TNF-α/IFN-γ-stimulation of iMCs resulted in a rapid increase in the mRNA expression of both IDO and cyclooxygenase (COX)-2, a key enzyme involved in the production of PGE$_2$ (Figure 2D). To analyse the role of IDO and PGE$_2$ in the iMCs-mediated inhibition of T cells, we added 1-MT (1-methyl tryptophan) and indomethacin, which are specific inhibitors of IDO and COX-1/2 activity, respectively (Figure 2E). We observed a small, but significant, reduction in the suppressive capacity

of the iMC in the presence of 1-MT (Figure 2F), but not with indomethacin (Figure 2G). Furthermore, the IDO activity was assessed in the cell cultures by determining the concentrations of tryptophan (Figure 2H, left graph) and its metabolite L-kynurenine (Figure 2H, middle graph) in the supernatants. We found that the IDO activity, as defined by the L-kynurenine/tryptophan ratio, was significantly increased in the PBMC:iMC co-cultures in comparison to PBMCs alone (Figure 2H, right graph). As expected, the addition of 1-MT significantly reduced the IDO activity. These data further suggest a role of iMC-derived IDO in their inhibition of T cell proliferation.
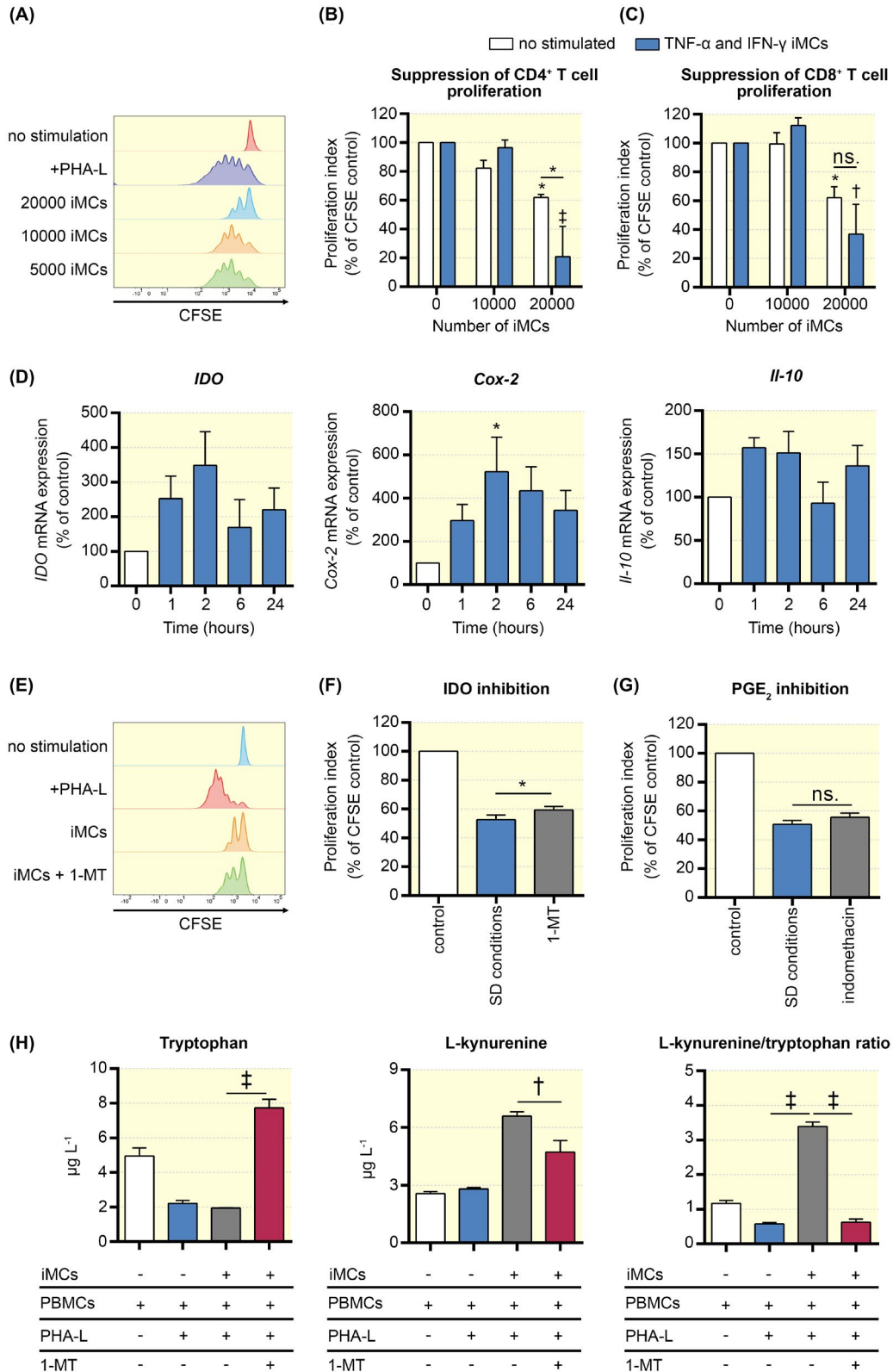
**FIGURE 2** iMCs inhibit T cell proliferation in vitro. CFSE-labeled PBMCs were stimulated with PHA-L in the presence or absence of increasing numbers of nonstimulated or TNF-α/IFN-γ pre-stimulated iMCs. Six days later, cells were acquired on a BD FACsAria™ IIIu cell sorter and the proliferation of CD4$^+$ and CD8$^+$ T cells was quantified using the FlowJo software. (A) Representative histograms showing CFSE-dilution of PHA-L-activated CD4$^+$ T cells cultured with or without nonstimulated iMCs. (B) Proliferation index of CD4$^+$ T cells cultured in the presence of nonstimulated (white bars) and TNF-α/IFN-γ pre-stimulated (blue bars) iMCs. Percentage of CFSE control refers to CFSE levels in PBMCs alone, stimulated with PHA-L at day 6. Data are shown as mean (SEM) of 3 independent experiments. $^*P < .05$ and $^‡P < .001$ vs "0 iMCs", $^*P < .05$. (C) Proliferation of CD8$^+$ T cells cultured in the presence of nonstimulated (white bars) and TNF-α/IFN-γ pre-stimulated (blue bars) iMCs. Data are shown as mean (SEM) of 3 independent experiments. $^*P < .05$ and $^†P < .01$ vs "0 iMCs". (D) iMCs were stimulated with TNF-α/IFN-γ for 1, 2, 6 and 24 h and mRNA expression of *IDO* (left graph), *Cox-2* (middle graph) and *il-10* (right graph) were measured by qPCR. Data are shown as mean (SEM) of three independent experiments. $^*P < .05$ vs "0". (E) Representative histograms showing CFSE-dilution of CD4$^+$ T cells cultured with 20 000 iMCs in the absence or presence of 1-MT. Proliferation index of CD4$^+$ T cells co-cultured with 20 000 iMCs under standard (SD) conditions (blue bars), or with the addition of (F) 1-MT, or (G) indomethacin (grey bars). Data are shown as mean (SEM) of 6 independent experiments. $^*P < .05$. (H) Supernatants from the cell cultures were collected on day 6 and the concentrations of tryptophan (left graph) and L-kynurenine (middle graph) were determined by UHPLC-MS/MS. After that, the L-kynurenine/tryptophan ratio (right graph) was calculated. Data are shown as mean (SEM) of 6 independent experiments

## 2.3 | iMCs inhibit the LPS-induced expression of TNF-α in THP-1 macrophages

To evaluate the effect of iMCs on macrophage function, we pretreated THP-1 macrophages with iMCs or their conditioned media (iMC-CM), and measured the expression of anti-inflammatory and pro-inflammatory cytokines upon lipopolysaccharide (LPS) stimulation. As shown in Figure 3, iMCs stimulated with LPS (1 µg mL$^{-1}$) secreted low concentrations of TNF-α, whereas TNF-α secretion from THP-1 cells was highly increased after LPS stimulation. In contrast, THP-1 cells cultured in the presence of iMCs or iMC-CM produced significantly less TNF-α upon LPS stimulation (Figure 3A). On the other hand, the expression levels of IL-10 were not found to be significantly different between the groups (Figure 3B). Furthermore, IFN-γ/TNF-α stimulation of iMCs resulted in the induction of several genes involved in the polarization of macrophages into anti-inflammatory M2 macrophages, including TNFα-stimulated gene-6 (TSG-6), hepatocyte growth factor (HGF) and IL-6,[19] suggesting their possible involvement in the observed reduction in TNF-α production by THP-1 cells (Figure 3C).

## 2.4 | Conditioned media from iMCs promotes in vitro wound healing

We next analysed the impact of iMC-CM on human NCM356 colonic epithelial cells migration/proliferation, using an in vitro scratch wound healing assay. We found that the wound closure, at 24 and 48 hours after wounding, was significantly accelerated in iMC-CM-treated wells when compared with the control (DMEM) (Figure 4A,B). In addition, we found that stimulation of iMCs with TNF-α/IFN-γ rapidly induced the gene expression of tumor progression locus-2 (TPL-2) (Figure 4C). These data are in agreement with the proposed

role of TPL-2 in maintaining epithelial cell homeostatic responses by increasing its proliferation.[20]

## 2.5 | iMCs ameliorate DSS-induced acute colitis

Once the immunosuppressive and wound-healing activities of iMCs were confirmed in vitro, we sought to analyse their effect in an experimental model of acute intestinal inflammation induced by DSS, which displays human IBD-like clinical, histopathological and immunological features. In this model, the DSS disrupts the intestinal epithelial barrier, resulting in the exposure of the submucosa to various luminal antigens and activation of the cells mainly involved in the innate immune response.[21] Oral administration of 3% (w/v) of DSS during five consecutive days resulted in a progressive increase in disease activity index (DAI) values, characterized by sustained weight loss and excretion of diarrhoeic/bleeding faeces. However, mice treated with a systemic administration of iMCs one day after the initiation of the DSS-treatment showed a reduced DAI score (Figure 5A), diminished body weight loss (Figure 5B), a less pronounced increase in spleen weight (Figure 5C) but with no apparent reduction in the colon weight/length ratio (Figure 5D). Nevertheless, the iMC-treated mice showed a significant reduction in the histological damage of the colon (Figure 5E). Representative images of the histological examination of colonic tissue stained with alcian blue, haematoxylin and eosin showed the effect of iMCs on DSS-induced colitis In the DSS group we could see changes in the mucosa with areas of ulceration (black arrow) on the epithelial layer, in addition to a lower number of goblet cells and depleted of mucins (yellow arrow), and an intense inflammatory cell infiltrate (white arrow). In the iMCs group we found an improvement of the colonic histology with a reduced area of ulceration, more abundance of
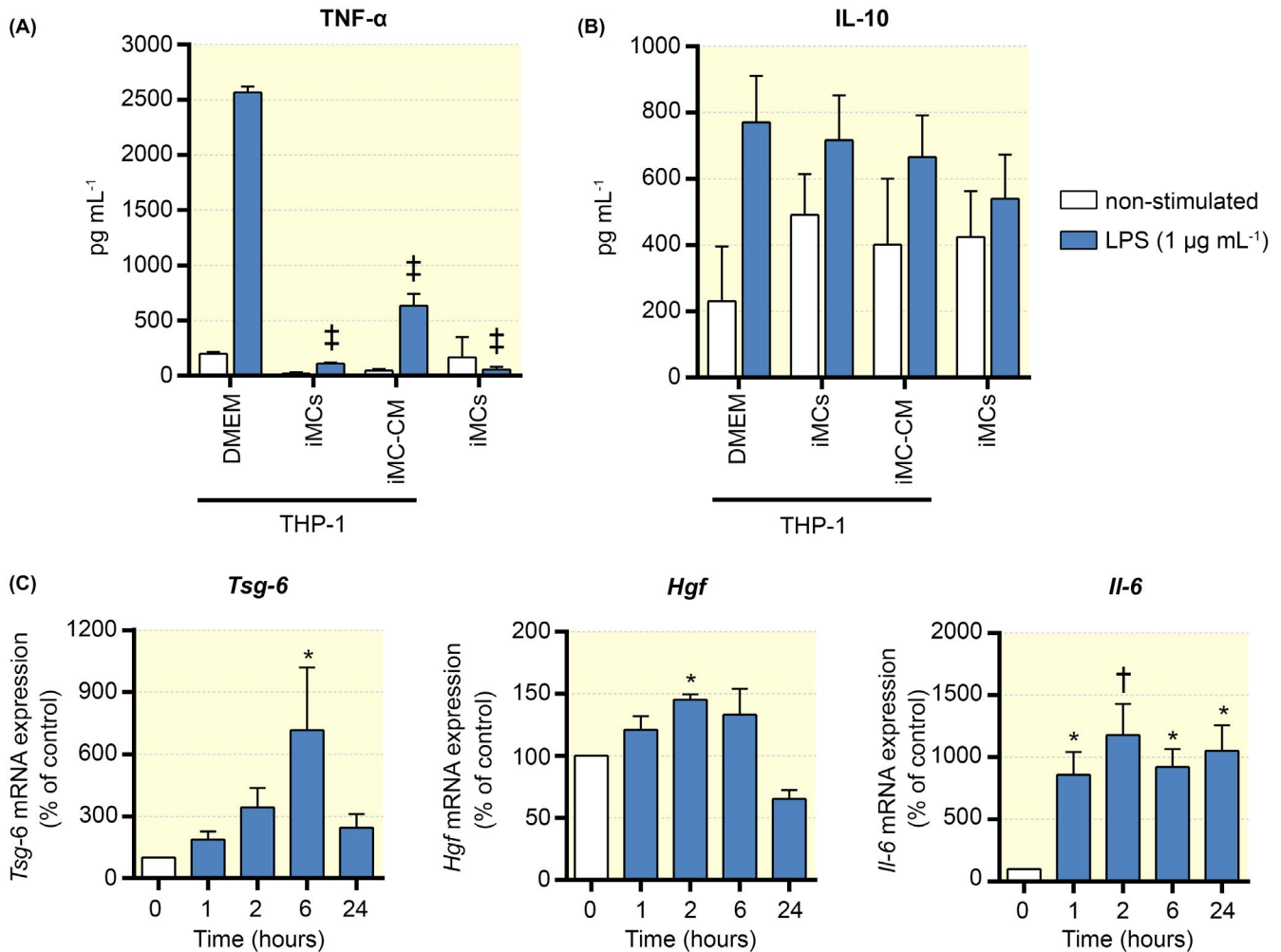
**(A)**

**TNF-α**



**(B)**

**IL-10**



☐ non-stimulated
■ LPS (1 µg mL⁻¹)

**(C)**

*Tsg-6*        *Hgf*        *Il-6*



**FIGURE 3** iMCs inhibit macrophage activation in vitro. PMA-activated THP-1 cells were cocultured with 100 000 iMCs or treated with iMC-CM for 48 h. Cells were subsequently cultured without (white bars) or with LPS (blue bars) for 24 h and the levels of TNF-α (A) and IL-10 (B) in the culture supernatants were analyzed by ELISA. $^{\ddagger}P < .001$ vs DMEM (+LPS) group. (C) iMCs were stimulated with TNF-α/IFN-γ for 1, 2, 6 and 24 h and mRNA expression of *Tsg-6* (left graph), *Hgf* (middle graph) and *Il-6* (right graph) was measured by qPCR. Data are shown as mean (SEM) of 3 independent experiments. $^{*}P < .05$, $^{\dagger}P < .01$ vs "0"

goblet cells and a diminished infiltration of inflammatory cells (Figure 5F).

## 2.6 | iMC administration protects the integrity of the intestinal barrier in DSS-treated mice

To characterize the effects of the iMCs on the impaired colonic epithelial permeability in colitic mice, intestinal barrier function was determined by oral administration of 4 kDa FITC-dextran. As shown in Figure 6A, colitic mice suffered a significant increase in intestinal permeability in comparison with the control group. However, this epithelial barrier impairment was significantly reduced in the iMCs-treated group. Additionally, the mRNA expression of proteins

involved in the maintenance of epithelial integrity, including zonula occludens-1 (*Zo-1*) and villin was significantly reduced in the DSS group in comparison with the control mice, whereas the iMC-administration significantly increased expression of these markers (Figure 6B,C). To further investigate the mechanisms behind this iMC-mediated protection of the intestinal barrier, we analysed the amount of proliferation (Ki67 immunofluorescence) and apoptosis (TUNEL assay) of cells in intestinal tissue sections from the control, DSS and DSS + iMCs groups. To our surprise, we found an increased number of Ki67⁺ cells in the DSS mice compared to the iMC-treated group, although the difference was not statistically significant (Figure 6D,E). In addition, the TUNEL assay showed a significant increase in apoptotic cells in the intestine of iMC-treated mice in comparison to DSS colitic mice (Figure 6E,G).
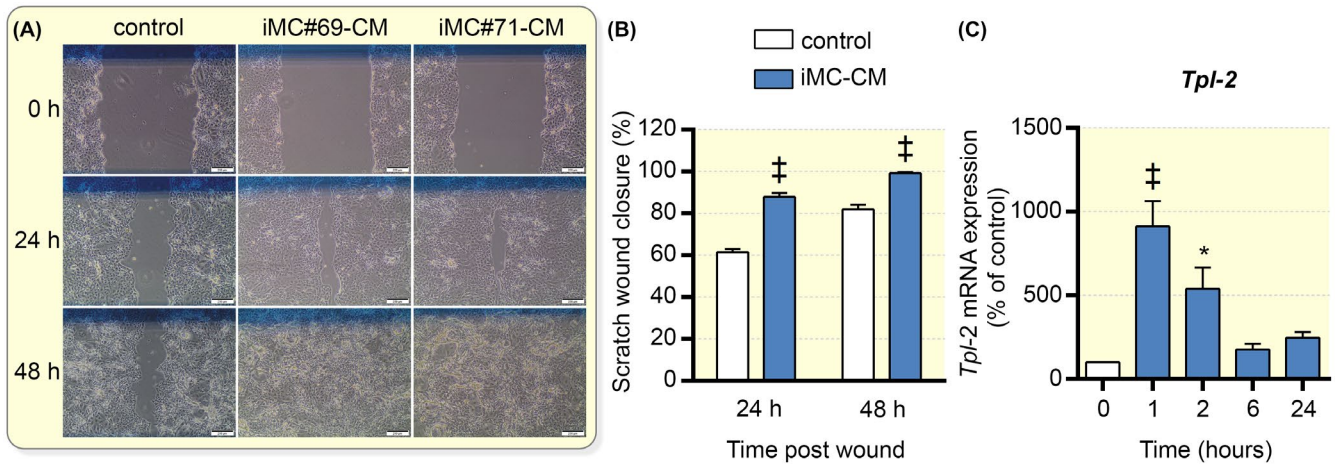
**FIGURE 4** iMC-conditioned medium (CM) promotes wound closure in the NCM356 human colonic epithelial cell scratch assay. (A) Representative phase contrast images of NCM356 epithelial cell layers cultured in DMEM (control) or iMC-CM from two individual donors (iMC#69, iMC#71) were taken at 0, 24 and 48 h after wounding (black line represents 200 µm). (B) Scratch wound closure was calculated as described in materials and methods. Data are shown as mean (SEM) of 4 independent experiments, $^{‡}P < .001$ vs control. (C) iMCs were stimulated with TNF-α/IFN-γ for 1, 2, 6 and 24 h and mRNA expression of *Tpl-2* was measured by qPCR. Data are shown as mean (SEM) of 3 independent experiments. $^{*}P < .05$, $^{‡}P < .001$ vs "0"

## 2.7 | iMC administration reduces inflammatory responses in colitic mice

The biochemical analysis of the colonic tissue corroborated the intestinal anti-inflammatory effect of iMCs, revealing the positive impact on the altered colonic immune response induced by DSS. DSS-induced colitis was characterized by increased expression of the pro-inflammatory cytokines *Tnf-α*, *Il-6* and *Il-12*, as well as the adhesion molecule *Icam-1*, and *Inos* (Figure 7A-E). iMC administration significantly reduced the expression of these cytokines, whereas only a trend in reducing *Icam-1* expression was observed (Figure 7D). We also analysed the expression of the M2 macrophage-related gene *ArgI* (Figure 7F). Although *ArgI* expression was highest in DSS-treated mice, the ratio *ArgI/Inos* was increased, albeit not significantly, in iMC-treated mice suggesting a possible polarization towards an anti-inflammatory M2 macrophage response (Figure 7G).[22] The intestinal anti-inflammatory activity exerted by iMCs was also corroborated when the pro-inflammatory inducible enzyme iNOS was evaluated by Western blot. In contrast to healthy control animals, mice from the DSS group showed an increased expression of this enzyme in colon. However, the systemic administration of iMCs significantly downregulated the colonic expression of iNOS (Figure 7H,I). Additionally, protein levels of the pro-inflammatory cytokine IL-1β were measured in culture supernatants of colonic explants by ELISA. IL-1β levels were significantly lower in the iMCs-treated colitic group when compared with the DSS control group (Figure 7J).

## 3 | DISCUSSION

In the intestine, epithelial cells and iMCs create a physical barrier, effectively separating the microbiome from the underlying tissues and immune system.[8] Although it is well documented that iMCs play important roles in intestinal health and disease, the true nature of their immunomodulatory capacity is not clear and warrants further research. The aim of the current study has been to characterize the tissue regenerative and immunomodulatory capacities of human iMCs in vitro and in vivo.

Evidence suggests that iMCs derived from bone marrow-derived gremlin$^+$ MSCs.[23] Although the phenotype of MSCs and their derivatives from different tissues is similar, their differentiation capacity, gene expression, and secretomes are distinct and partly reflect their tissue/organ-specific function.[24,25] Importantly, MSCs and iMCs retain their tissue specific characteristics through multiple passages in vitro[26,27] making it feasible to study, at least to some extent, their tissue-specific properties in vitro. In our study, we have isolated iMCs based on plastic adherence, resulting in the selection of a heterogeneous collection of fibroblastic cells, including fibroblasts and myofibroblasts. After 2-3 passages in vitro these cells adopted a homogenous phenotype (CD31$^−$CD34$^−$EpCam$^−$CD45$^−$CD73$^+$CD90$^+$CD105$^+$), similar to that of MSCs from bone marrow and adipose tissue,[28,29] which was maintained in culture upon serial passaging.

Several reports have shown a role of human iMCs in intestinal immune tolerance. Firstly, human colonic myofibroblasts promote intestinal tolerance through the expansion
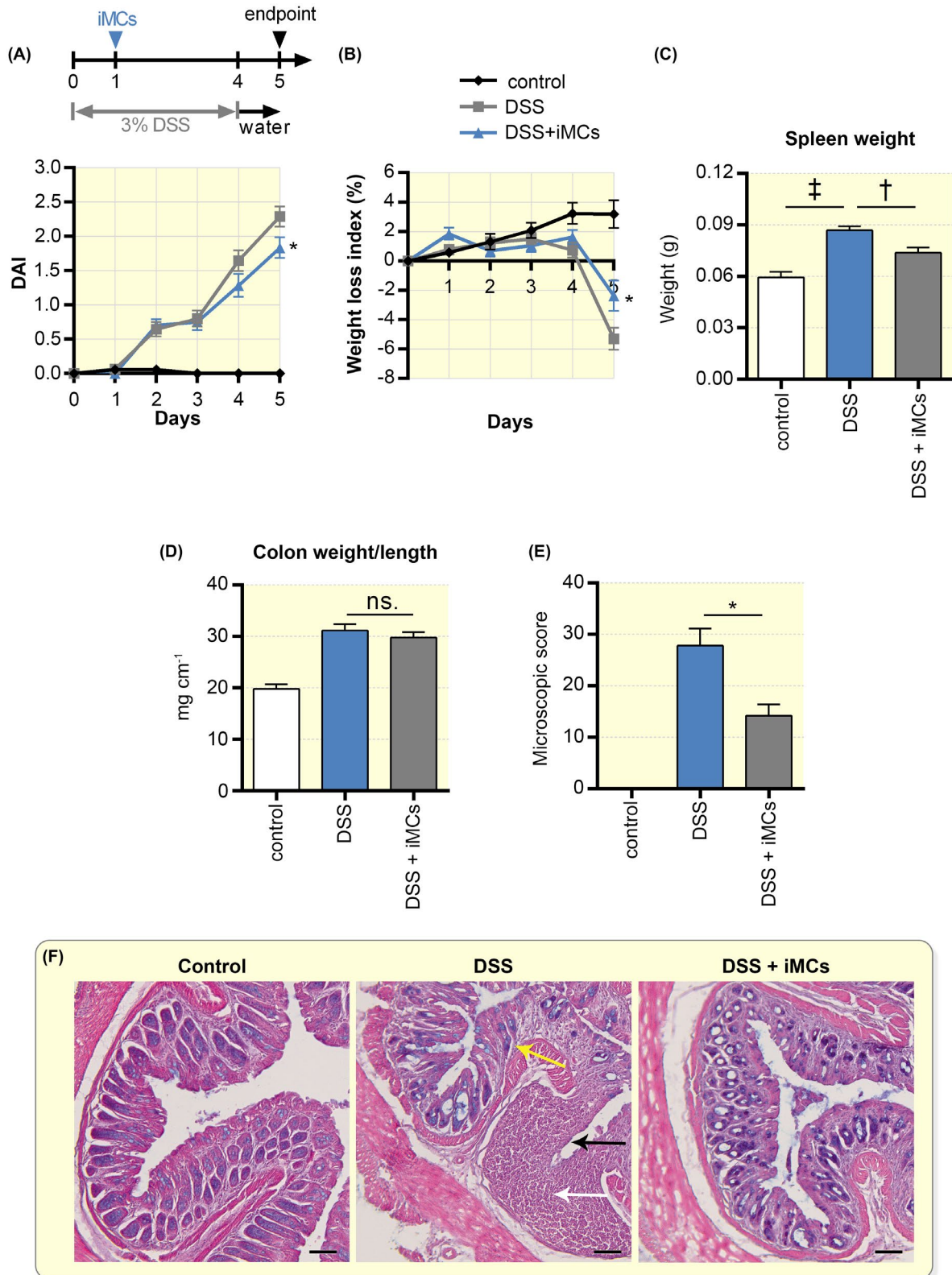
**FIGURE 5** Treatment with iMCs ameliorates DSS-induced acute colitis. Mice (n = 10) received 3% DSS in the drinking water ad libitum from day 0 to day 4. iMCs ($10^6$/mouse) were injected intraperitoneally (n = 10) on day 1. Mice receiving tap water were used as controls (n = 10). (A) Disease activity index (DAI) and (B) weight loss index was determined daily. (C) Spleen weight was determined on day 5. (D) Colon length/weight ratios determined on day 5. (E) Histological evaluation of control, DSS and iMC-treated mice. Data are shown as mean (SEM) of 5-6 individual mice/group. $^*P < .05$ vs DSS mice. (F) Representative histological images of colonic tissue stained with alcian blue (mucins), haematoxylin and eosin showing the effect of iMCs on DSS-induced colitis (the black arrow indicates areas of ulceration, the yellow arrow indicates the loss of goblet cells and decrease in mucins, and the white arrow indicates an intense inflammatory cell infiltrate)
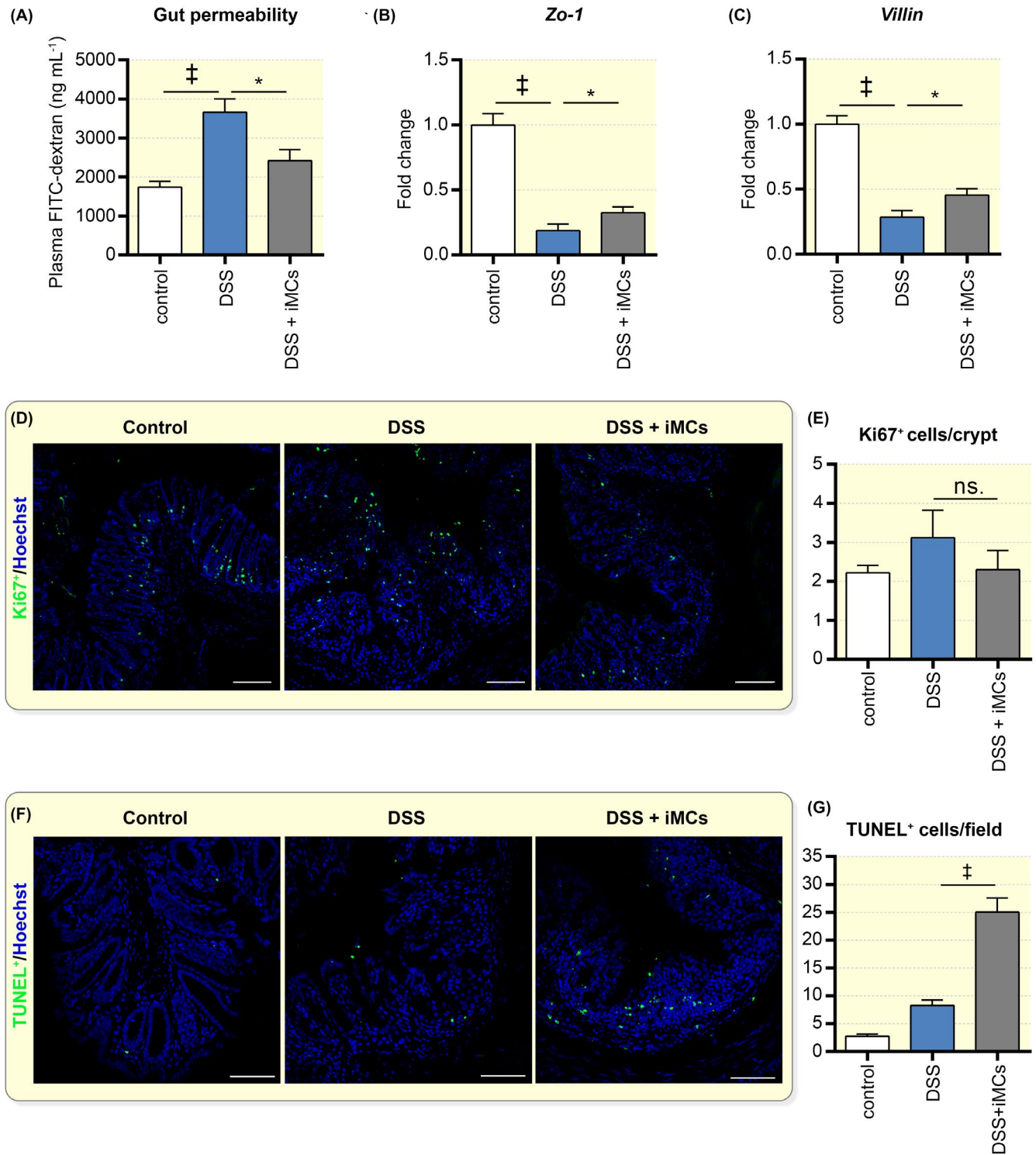
**FIGURE 6** iMCs promote the integrity of the intestinal epithelial barrier in colitic mice. (A) Gut permeability was determined on day 5 by measuring the plasma concentration of FITC-dextran. Expression of the epithelial integrity proteins (B) *Zonula occludens*-1 (*Zo-1*) and (C) *Villin* was quantified by qPCR. Fold-changes are expressed as mean (SEM). $^*P < .05$, $^†P < .01$, $^‡P < .001$ vs DSS mice. (D) Representative images showing immunofluorescence staining of Ki67 (proliferation) in colonic tissue sections. Ki67+ cells are shown in green and nuclei are shown in blue (Hoechst). White bars represent 100 μm. (E) Data show Ki67+ cells/crypt and are represented as mean (SEM) of 5 mice/group. ns., not significant. (F) Representative images of TUNEL-stained (apoptosis) colonic tissue sections from control, DSS and iMCs-treated mice. Apoptotic cells are stained in green and nuclei in blue (Hoechst). (G) Data show TUNEL+ cells/field, and are represented as mean (SEM) of 5 mice/group. $^‡P < .001$ vs DSS mice
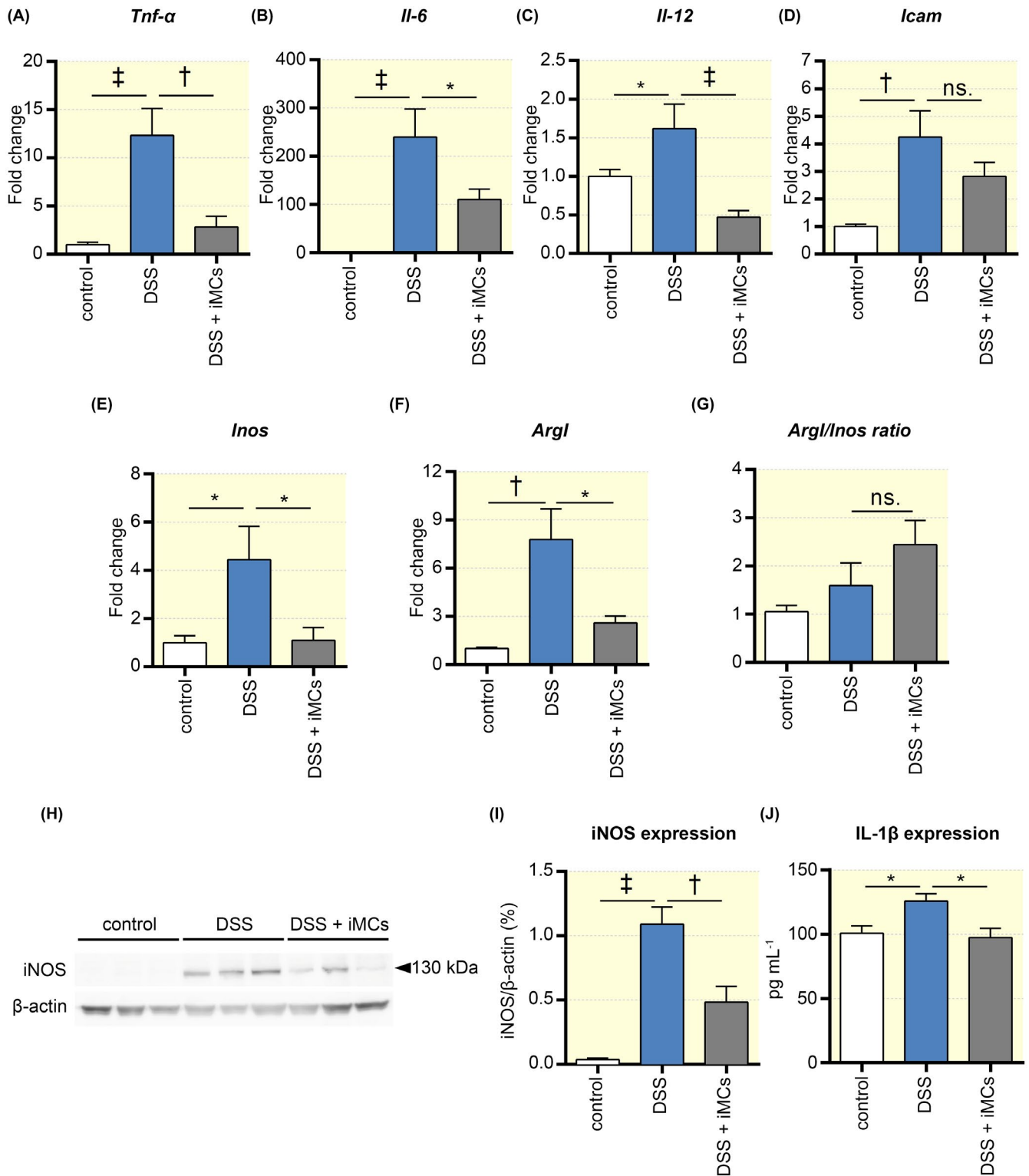
**FIGURE 7** iMCs inhibit DSS-induced inflammation in colitic mice. Total RNA was extracted from colons of control, DSS- and iMC-treated mice on day 5 and the gene expression of (A) *Tnf*-α, (B) *Il-6*, (C) *Il-12*, (D) *Icam*, (E) *Inos* and (F) *ArgI* were analyzed by qPCR. $^{*}P < .05$, $^{†}P < .01$, $^{‡}P < .001$ vs DSS mice. (G) Based on the qPCR results, the *ArgI/Inos* ratio was calculated. Data are shown as mean (SEM) of 10 mice/group of two separate experiments. (H) Colonic iNOS protein expression was evaluated by Western blot. The arrow indicates the iNOS monomer with a molecular mass of 130 kDa. (I) Densitometric analysis of the corresponding bands. (J) IL-1β protein levels in culture supernatants of colonic explants from control, DSS-, and iMC-treated mice were measured by ELISA. $^{*}P < .05$ vs DSS mice

of CD4$^+$CD25$^{high}$Foxp3$^+$ regulatory T cells.[30] Secondly, human colonic CD90$^+$ stromal cells express PD-L1 and PD-L2 which they use to suppress the proliferation of CD45RA$^+$CD4$^+$ T cells in a cell contact–dependent manner.[28] We found that iMCs could inhibit the proliferation of PBMCs (both CD4$^+$ and CD8$^+$ T cells) induced by PHA-L. Pre-stimulation of iMCs with TNF-α and IFN-γ increased their immunosuppressive capacity in vitro, which correlated with an induction of *Ido1* mRNA expression. Furthermore, we found a significant increase in IDO enzyme activity in the PBMC:iMC co-cultures. IDO is a well-known IFN-γ-inducible inhibitor of T cell proliferation used by human bone marrow MSCs.[31] In IBD, IDO is highly up-regulated in the inflamed intestinal mucosa and TLR9-mediated induction of IDO protects against experimental colitis.[32] However, to our knowledge, no study has analysed the function of IDO in iMCs. Our data demonstrate that iMCs can use IDO to inhibit T cell proliferation. However, the inhibition of IDO did not result in a complete reversion of suppression, indicating that iMCs use additional mechanisms to inhibit T cell responses. Interestingly, we found that some iMC cell lines depended to a higher degree on IDO, suggesting that their immunomodulatory capacity and its underlying mechanisms vary with donor, and most likely, experimental conditions.[33]

Although iMCs have been shown to promote mucosal tolerance, several reports have highlighted a pro-inflammatory role of iMCs in IBD. Kinchen and colleagues observed a remodeling of the colonic mesenchyme in IBD patients characterized by the emergence of a pro-inflammatory iMC population which prevented epithelial healing and promoted disease.[13] Furthermore, West and colleagues showed that oncostatin M (OCM) is up-regulated in IBD patients compared to healthy controls which induces a pro-inflammatory response in intestinal stromal cells.[34] Importantly, high levels of OCM correlated with a decreased responsiveness to anti-TNF-α therapy. Recently, Martin et al,[35] and Smillie et al[36] characterized inflammatory cell modules in the affected intestinal mucosa of CD and UC patients which associate with resistance to anti-TNF-α therapy. In addition to epithelial and immune cells, these modules contained inflammatory iMCs with the ability to recruit monocytes to the site of inflammation. Monocytes/macrophages play important roles in the pathogenesis of IBD[37] and recent data suggest that anti-TNF-α monoclonal antibodies exert their beneficial effect on IBD through the induction of immunomodulatory macrophages.[38] Bone marrow and adipose tissue-derived MSCs have previously been shown to induce anti-inflammatory macrophages which ameliorate experimental sepsis and colitis.[39,40] However, few studies have analysed the effect of human iMCs on macrophage polarization[41] and to this end we employed the human leukemia monocytic THP-1 cell line which is an adequate model for analysing macrophage polarization into the M1 and M2 activation states.[42,43] We

show that iMCs as well as their conditioned medium inhibited the LPS-induced production of TNF-α by THP-1-derived macrophages. How iMCs reduce the production of TNF-α by THP-1 macrophages is not known. We found that TNF-α/IFN-γ induced the expression of several genes involved in the polarization of M2 macrophages, including TSG-6, HGF and IL-6.[19] However, additional studies are necessary to specifically evaluate the involvement of these factors in the immunomodulatory function of iMCs. Further insight into how iMC can induce anti-inflammatory macrophages could help in re-educating the inflammatory iMC populations that appear in IBD patients.

Due to the dual role of iMCs in regulating immune responses we decided to analyse the anti-inflammatory and epithelial regenerative capacity of iMC in vivo, using the DSS-model of acute intestinal inflammation in C57BL/6J mice. This experimental model resembles the main manifestations of IBD, concretely this model has been used to study the innate immune mechanisms in intestinal inflammation and simulates human IBD by promoting an exaggerated Th2 immune response.[44] We injected the iMCs intraperitoneally since this route has proven the most adequate based on therapeutic efficacy and migration of MSCs towards the inflamed intestine.[45,46] We show for the first time that injection of iMC, one day after the start of DSS administration, significantly decreased the colitis severity and weight loss. Injection of iMCs resulted in a reduction of colonic inflammation, evidenced by a decreased immune infiltration and down-regulation of inflammatory mediators in the colon. In addition, we observed an increment, although not significant, in the *ArgI/Inos* ratio, suggesting a polarization of macrophages towards an M2 response, which is in agreement with our in vitro results using THP-1 cells. These data are in accordance with the anti-inflammatory effects seen using MSCs from different tissues in experimental colitis[47] and again shows that iMCs from the healthy intestine possess immunomodulatory capacity.

We found that administration of iMCs protected the intestinal epithelial barrier against the DSS-induced damage, which is in agreement with our observation that the iMC-CM can promote wound regeneration in vitro. This is also supported by recent studies demonstrating that murine CD90$^+$CD34$^+$gp38$^+$ iMCs are important for the maintenance of intestinal epithelial stem cells.[48,49] One possible mediator providing this protection could be PGE$_2$ which is known to stimulate epithelial growth, inhibit epithelial apoptosis during insults and potentiate WNT-signaling.[50,51] However, we found higher levels of proliferating (Ki67$^+$) cells in the colons of DSS mice compared to iMC-treated mice which is in contrast to studies showing an increased intestinal epithelial proliferation after MSC administration to colitic mice.[52] Nevertheless, several studies have demonstrated that DSS-induced epithelial damage is followed by a compensatory increase in epithelial cell proliferation.[53-56] Consequently, our

data suggests that, in our experiments, iMC administration does not promote intestinal barrier integrity by promoting epithelial cell proliferation, but rather protecting against DSS-induced tissue damage.

We thus proceeded to evaluate the extent of apoptosis in the colonic tissue in our experimental groups. Although there was an increase in TUNEL-positive/apoptotic cells between healthy and DSS-treated mice, we unexpectedly found a significantly higher number of TUNEL-positive cells in the iMC-treated group compared to DSS mice. Although surprising, this is in agreement with several studies demonstrating that MSCs, via IDO[57] or FAS-L[58] can induce apoptosis of T cells, playing a pivotal role in their ability to ameliorate colitis.[58,59] In addition, it has also been reported that MSC-derived membrane particles can induce selective apoptosis of pro-inflammatory monocytes.[60] Although our data show that iMC administration results in a clear improvement of the integrity of the intestinal barrier in colitic mice, further investigations are needed to understand the mechanisms behind this observation.

Interestingly, several recent studies have shown that BM-MSCs can be polarized into pro-inflammatory "MSC1" or anti-inflammatory "MSC2" phenotypes when primed via TLR4 and TLR3, respectively.[61,62] Regarding iMCs, Beswick recently reported that the expression of PD-L1 on iMCs in CD decreases, making them unable to efficiently control the pathogenic Th1 responses. Furthermore, TLR4 signaling increased the PD-L1-dependent inhibition of T cells by iMCs.[10] These data suggest that the microbiota can modulate both the tissue regenerative and immunomodulatory capacity of iMCs. As the dysbiotic microbiome seen in IBD patients has been shown to drive IBD pathogenesis, further studies should investigate its effect on immunomodulatory properties of iMC.

In summary, we have shown that iMCs isolated from healthy human intestine promote epithelial wound closure and possess the capacity to modulate immune/inflammatory responses in vitro and in vivo. Our data might be relevant for the development of new therapies targeting the dysregulated intestinal stroma in IBD.

# 4 | MATERIALS AND METHODS

## 4.1 | Cell isolation and cultures

Intestinal resections were obtained from patients undergoing surgery in the University Hospital Virgen de las Nieves (Granada, Spain). These patients had been previously admitted for bowel resection due to various intestinal pathologies, including diverticulitis, benign polyps or colon cancer. iMCs were isolated from noncomprised tissue (ie tissue that distances a minimum of 5 cm from the affected area). All the samples were collected with the written consent of each patient according to the Declaration of Helsinki. The study was approved by the local ethics committee and conforms with good publishing practice in physiology.[63]

Freshly isolated intestinal resections were washed thrice with PBS supplemented with 2% penicillin/streptomycin to remove debris, stools, and erythrocytes. The tissue was weighed, cut into small pieces and resuspended in 15 mL of HBSS (40-50 mg tissue mL$^{-1}$) containing 400 U mL$^{-1}$ DNase (Sigma-Aldrich), 500 U mL$^{-1}$ collagenase type IV (Sigma-Aldrich) and 0.09 U mL$^{-1}$ dispase II (Roche Applied System) and incubated for 60 minutes at 37ºC. The digest was washed thrice with cold PBS containing 2 mM EDTA and filtered through a 70-µm and a 100-µm nylon mesh. Finally, cells were resuspended in complete DMEM Advanced (Gibco, ThermoFisher Scientific) (containing 10% fetal bovine serum, 2 mM Ultraglutamine (Lonza), 1% penicillin/streptomycin and 1% amphotericin B) and cultured at 37ºC and 5% $CO_2$. Nonadherent cells were removed after 24 hours in culture. Adherent cells showed a fibroblast-like morphology and were passed to a new culture flask when cultures reached 90% confluence. Cells were used at passage 1-8.

## 4.2 | Immunophenotypic characterization of iMCs

iMCs at passage number 1-3 and later on at passage number 7-8 were harvested using TrypLE (ThermoFisher Scientific), washed with PBS and incubated (20 000-30 000 cells/staining) with 7-aminoactinomycin D (7-AAD) (Nalgene, Nalgen Nunc International Corporation) and FcR blocking reagent (Miltenyi Biotec GmbH) for 15 minutes at 4ºC. Cells were subsequently stained with the following antibodies: CD45-APC-eFluor®780, CD73-PE, CD90-FITC, CD105-Pe-Cy7 (eBioscience, ThermoFisher Scientific), CD31-FITC, EpCam-PerCP-Cy5.5, CD34-APC and PD-L1/CD274-PE (BD Biosciences) for 30 minutes at 4ºC. Corresponding isotype antibodies were used to evaluate background staining. Data were acquired using the BD FACS Canto II flow cytometer (BD Biosciences) and analysed using the Flowjo v10.6.2 software (FlowJo LLC).

## 4.3 | T cell suppression assay

iMCs were harvested, treated with mitomycin C (50 µg mL$^{-1}$, Sigma-Aldrich) for 20 minutes at 37ºC and plated at 10 000 and 20 000 cells/well in flat bottomed 96-well plates. Cells were subsequently cultured with or without 3 ng mL$^{-1}$ TNF-α (Peprotech EC Ltd) and 10 ng mL$^{-1}$ IFN-γ (Peprotech EC Ltd) for 24 hours. After that, PBMCs were isolated using Lymphoprep™ (StemCell Technologies) and labelled with

5 μM CFSE (Sigma-Aldrich) for 12 minutes at 37ºC. Labelled PBMCs (200 000 cells/well) and 2.5 μg mL$^{-1}$ of the T cell mitogen PHA-L (eBioscience, ThermoFisher Scientific) were added to the iMC cultures. In some experiments, 1-MT (1 mM, Sigma-Aldrich) or indomethacin (20 μM, Sigma-Aldrich) were added to the cocultures. On day 6, supernatants were collected and PBMCs were carefully harvested and stained with anti-CD4-PE (BD Biosciences), anti-CD3-APC (BioLegend) and Zombie Aqua™ (BioLegend) as viability dye. Labelled cells were acquired on a BD FACsAria™ IIIu cell sorter (BD Biosciences) and the cell division (proliferation index based on CFSE signal intensity) of CD4$^+$ and CD8$^+$ (CD3$^+$CD4$^-$) T cells was analysed using the FlowJo v10.6.2 software (FlowJo LLC; Becton, Dickinson and Company).

## 4.4 | Detection of indoleamine 2,3-dioxygenase activity by UHPLC–MS/MS in conditioned PBMC:iMC supernatants

IDO activity was evaluated by quantifying tryptophan and L-kynurenine concentrations in supernatants from the PBMC:iMC-cultures on day 6 by UHPLC-MS/MS. All chemicals used for quantification were of analytical HPLC-MS grade. Water was obtained by purification with a Milli-Q system from Millipore. Formic acid and acetonitrile for mobile phases were purchased from Scharlab.

UHPLC-MS/MS analysis was performed on a Waters Acquity UPLC™ H-Class from Waters. A Xevo TQS tandem quadrupole mass spectrometer (Waters) equipped with an orthogonal Z-spray™ electrospray ionization (ESI) source was used for tryptophan and L-kynurenine detection. Separation of compounds was obtained with a BEH (Ethylene Bridged Hybrid) column C18 50*2.7 mm 1.7 μm particle size (Waters). The compounds were separated using a gradient mobile phase consisting of solvent A (LC-MS grade water plus 0.1% of formic acid) and solvent B (LC-MS grade acetonitrile plus 0.1% formic acid). Thus, the elution program was a multi-step linear gradient at a flow rate of 0.55 mL min$^{-1}$. Gradient conditions were 0.0-3.0 minutes 1% phase B; 3.0-5.0 minutes, 10%-25% phase B; 5.0-7.0 minutes, 25%-90% phase B and back to 1% in 0.1 minutes. Total run time was 11.0 minutes. The injection volume was 10 μL and the column temperature was maintained at 45ºC.

For mass spectrometric analysis, ESI was performed in positive ion mode. The tandem mass spectrometer was operated in the multiple reactions monitoring (MRM) mode. Instrument parameters were as follows: capillary voltage, 2.00 kV; source temperature, 150ºC; desolvation temperature, 600ºC; cone gas flow, 150 L h$^{-1}$; desolvation gas flow, 1000 L h$^{-1}$; collision gas flow, 0.15 mL min$^{-1}$, and nebulizer gas flow, 7.0 bar. Dwell time was set at 25 ms collision energies and cone voltages were optimized for both analytes.

In order to quantify the individual content of the analytes, two calibration curves were prepared using tryptophan and L-kynurenine commercial standards (Sigma-Aldrich). Concentrations were determined by interpolation in the corresponding calibration curve using the peak area. MassLynx 4.1 software was used for instrument control, peak detection and integration.

## 4.5 | Preparation of the conditioned media of iMCs

iMCs from four unrelated donors were seeded in 24-well plates at a density of 50 000 cells mL$^{-1}$. Once they reached confluence, the medium was replaced with fresh basal medium and incubated for 48 hours at 37ºC at 5% $CO_2$. The iMC-CM were harvested, centrifuged at 500×$g$, aliquoted and stored at −20ºC until use.

## 4.6 | Anti-inflammatory effect of iMCs and their conditioned media in THP-1 cells

The human monocytic cell line THP-1 was maintained in complete RPMI 1640 (Gibco; Thermofisher Scientific). For co-culture experiments, THP-1 cells (250 000 cells mL$^{-1}$) were first differentiated into adherent macrophages with 50 ng mL$^{-1}$ of PMA (Sigma-Aldrich) in 24-well plates. After 48 hours, human iMCs (100 000 cells) or iMC-CM were added to the adherent THP-1 macrophages. After 48 hours, cells were stimulated with LPS (1 μg mL$^{-1}$; Sigma-Aldrich) for another 24 hours. Supernatants were collected for cytokine determination by ELISA.

## 4.7 | Scratch wound healing assay

NCM356 human colonic epithelial cells were kindly provided by Laura Medrano González and Ezra Aksoy (William Harvey Research Institute, Queen Mary University of London, London, UK). Cells were seeded at 150 000 cells mL$^{-1}$ in 6-well plates. When the cultures had reached confluence, the monolayers were scraped in straight lines using sterile 200 μL pipette tips in order to create scratch wounds of homogenous width. After a wash with PBS, cells were cultured in control or conditioned media, both diluted 1:1 with fresh basal medium. To track the scratch-wound closure, the scratches were observed by an inverted microscope (Olympus-CKX41, Olympus Europa SE & Co. KG) and equivalent photos were taken at 0, 24 and 48 hours. Finally, the scratch area was measured using the ImageJ software (Free Software Foundation Inc). These experiments were performed with iMC-CM prepared from iMCs of 4 different donors.

## 4.8 | Induction of colitis with DSS

All animal studies were carried out in accordance with the "Guide for the Care and Use of Laboratory Animals" as promulgated by the National Institute of Health and the protocols approved by the Ethic Committee of Laboratory Animals of the University of Granada (Spain) (CEEA 17/09/2019/156). All the animals were housed in makrolon cages, maintained in an air-conditioned atmosphere with a 12-hour light-dark cycle and provided with free access to tap water and food. Acute colitis was induced in male C57BL/6J mice (7-9 weeks old) (Charles River) by adding 3% DSS (36-50 KDa, MP Biomedicals) from day 0 to day 4 in the drinking water. On day 1, mice were injected intraperitoneally (i.p.) with $1 \times 10^6$ human iMCs in 200 μL PBS. The control and DSS groups received i.p. injections of 200 μL sterile $1 \times$ PBS. Mice were euthanized on day 5.

## 4.9 | Determination of DAI in DSS-induced colitis

The DAI (scale 0-4) was determined daily by evaluating weight loss, stool consistency, and presence of fecal blood in each mouse by a blind observer. A score was assigned to each one of these parameters according to the criteria previously proposed.[64] Once the animals were euthanized, the colons were aseptically removed, rinsed with PBS, weighed, and its length was measured under a constant load (2 g). The colonic tissue was then sectioned in different fragments for subsequent histological and immunological evaluation.

## 4.10 | In vivo intestinal permeability

The day before sacrifice, mice from the different experimental groups (n = 8/group) were fasted for 12 hours and administered FITC-dextran 4 (Sigma-Aldrich) by oral gavage (350 mg kg$^{-1}$ body weight). Four hours after administration, just before sacrifice, blood was drawn via intracardiac puncture and centrifuged at $4000 \times g$ for 10 minutes at 4ºC. Plasma was diluted (1:10) in PBS and analysed for FITC-dextran concentration with a fluorescence spectrophotometer (Fluorostart, BMG Lab Technologies) at an excitation wavelength of 485 nm and emission wavelength of 535 nm. A standard curve was obtained by serial dilutions of FITC-dextran (Sigma-Aldrich) in PBS.[65]

## 4.11 | Histological studies

Representative colonic specimens were taken 1 cm from the rectum, fixed in 4% paraformaldehyde (PFA), dehydrated in 15% and 30% sucrose and embedded in OCT. Histochemical staining of mucins was performed by incubation of 8 μm sections in alcian blue (1%) in acetic acid (3%) for 30 minutes prior to conventional hematoxylin and eosin staining. Histological damage was evaluated by a blind observer according to a previously established scoring system which takes into account the presence of ulceration, immune cell infiltration, edema and the condition of the crypts.[66]

## 4.12 | Assessment of proliferation and apoptosis by immunofluorescence

To determine proliferation, cryosections of PFA-fixed OCT-included colonic tissue were used to detect Ki67 positive cells. Permeabilization and blocking of the samples was performed with a solution of 0.1% saponin, 0.05% sodium azide and 1% BSA (all from Sigma-Aldrich) in PBS for 1 hour at room temperature. Then, slides were probed with primary polyclonal rabbit anti-Ki67 antibody (1:500 dilution in blocking buffer, catalog# ab64693 [Abcam]) at 4ºC overnight. An anti-rabbit AF488-conjugated secondary antibody (1:1000 dilution catalog# ab150077 [Abcam]) was used for signal amplification and detection. Hoechst 33342 (Invitrogen, ThermoFisher Scientific) was used to stain the nuclei. Anti-rabbit IgG isotype control (catalog# 02-6102, Invitrogen, ThermoFisher Scientific) was used as negative control. Images were acquired with a Nikon Eclipse Ti-E A1 confocal microscope (Centre for Scientific Instrumentation, University of Granada) equipped with a 20× objective.

Apoptosis was evaluated using the DeadEnd Fluorometric TUNEL system (Promega) in colonic tissue sections following the manufacturer's indications. Hoechst 33 342 (Invitrogen, ThermoFisher Scientific) was used to stain the nuclei. Images were acquired with a Leica TCS-SP5 II spectral multiphoton confocal microscope (Centre for Scientific Instrumentation, University of Granada) equipped with a 20× objective. In both cases, acquisition of green channel (positive signals) was performed using the 488 nm laser and 505-550 nm emission filter. Quantification of Ki67$^+$ cells per crypt and TUNEL$^+$ per field was done using 15 random crypts or 5 random fields per slide, respectively. Images were analysed with ImageJ software (Free Software Foundation Inc).

## 4.13 | Colonic explant culture and cytokine determination by ELISA

Three whole thick colonic punch biopsies (Miltex) were obtained from distal, medial and proximal regions and incubated in 0.5 mL of complete DMEM for 24 hours. After that, supernatants were collected and IL-1β concentration (pg mL$^{-1}$) was measured by ELISA (PeproTech EC Ltd).

**TABLE 1** RT-qPCR primer sequences

| Gene name | Primer sequence 5′→3′ | Species | Annealing $T$ (ºC) | RefSeq accession number |
|---|---|---|---|---|
| *Gapdh* | FW 5′-CCATCACCATCTTCCAGGAG<br>RV 5′-CCTGCTTCACCACCTTCTTG | Mouse/human | 60 | NM_001289726.1 |
| *Zo-1* | FW 5′-GGGGCCTACACTGATCAAGA<br>RV 5′-TGGAGATGAGGCTTCTGCTT | Mouse | 56 | NM_009386.2 |
| *Villin* | FW 5′-CTCCGAGCAGATTGAGAAGG<br>RV 5′-GGTGCTGCCACTCTTCTACC | Mouse | 60 | NM_009510.2 |
| *Inos* | FW 5′-GTTGAAGACTGAGACTCTGG<br>RV 5′-GACTAGGCTACTCCGTGGA | Mouse | 56 | NM_010927.4 |
| *Tnf-α* | FW 5′-AACTAGTGGTGCCAGCCGAT<br>RV 5′-CTTCACAGAGCAATGACTCC | Mouse | 56 | NM_001278601.1 |
| *Il-6* | FW 5′-TAGTCCTTCCTACCCCAATTTCC<br>RV 5′-TTGGTCCTTAGCCACTCCTTC | Mouse | 60 | NM_031168.2 |
| *Icam-1* | FW 5′-GAGGAGGTGAATGTATAAGTTATG<br>RV 5'-GGATGTGGAGGAGCAGAG | Mouse | 60 | NM_010493.3 |
| *Il-12* | FW 5'-CATCGATGAGCTGATGCAGT<br>RV 5'-CAGATAGCCCATCACCCTGT | Mouse | 59 | NM_008351.3 |
| *Arg1* | FW 5'-TTGCGAGACGTAGACCCTGG<br>RV 5'-CAAAGCTCAGGTGAATCGGC | Mouse | 63 | NM_007482.3 |
| *Cox-2* | FW 5'-AAGCAGGCTAATACTGATAGG<br>RV 5'-TGTTGAAAAGTAGTTCTGGG | Mouse | 56 | NM_000963.4 |
| *IDO1* | FW 5'-TTGTTCTCATTTCGTGATGG<br>RV 5'-TACTTTGATTGCAGAAGCAG | Human | 56 | NM_002164.6 |
| *Il-10* | FW 5'-TGGTGAAACCCCGTCTCTAC<br>RV 5'-CTGGAGTACAGGGGCATGAT | Human | 60 | NM_001382624.1 |
| *Tsg-6* | FW 5'-CCAAATGAGTACGAAGATAACC<br>RV 5'-CACAGTATCTTCCCACAAAG | Human | 55 | NM_007115.4 |
| *Hgf* | FW 5'-GCAATTTTTGGTTTGGCTGT<br>RV 5'-CCTGCCCACAGCATATAGGT | Human | 60 | NM_001010932.3 |
| *Il-6* | FW 5'-GCAGAAAAAGGCAAAGAATC<br>RV 5'-CTACATTTGCCGAAGAGC | Human | 55 | NM_001371096.1 |
| *Tpl-2* | FW 5'-AACATTGCTGATTCTTCGTG<br>RV 5'-CCCGAACAAGATTGAAGTAG | Human | 55 | NM_001320961.2 |

## 4.14 | Western blot

Representative colonic samples (n = 6) were processed as described previously to evaluate iNOS expression by Western blotting. Briefly, colonic samples were homogenized (1/5 w/v) in PBS supplemented with 0.1% sodium dodecyl sulfate (SDS), 0.1% sodium deoxycholate, 1% Triton X-100 and protease and phosphatase inhibitors (aprotinin, leupeptin and PMSF) (Sigma-Aldrich). Then, 100 μg of protein were boiled at 95ºC in 4× Laemmli sample buffer (BioRad) and resolved by sodium dodecyl sulphate-polyacrylamide gel electrophoresis (SDS-PAGE, 10% polyacrylamide under reducing conditions) and electro-transferred to a PVDF membrane (GE Healthcare Life Sciences). Membranes were blocked with 3% BSA and probed with anti-iNOS (Transduction Laboratories, BD Biosciences) at 1:500 dilution, 4ºC overnight, followed by 1 hour of incubation with peroxidase-conjugated anti-rabbit IgG antibody (1:5000 dilution) (Sigma-Aldrich) and finally detected with the Western Lightning™ Chemiluminescence Reagent Plus (PerkinElmer Spain SL). Control of protein loading and transfer was conducted by detection of β-actin levels.[66] The quantification of bands was performed by densitometric analysis using ImageJ software (Free Software Foundation Inc).

## 4.15 | Analysis of gene expression by RT-qPCR

To analyse the effect of proinflammatory cytokines on the expression of immunomodulatory mediators by iMCs, cells were cultured with or without TNF-α (3 ng mL$^{-1}$, Peprotech EC Ltd) and IFN-γ (10 ng mL$^{-1}$, Peprotech EC Ltd) for 1, 2,

6 and 24 hours. Total RNA was extracted using NucleoZOL (Macherey-Nagel) following the manufacturer's instructions, and reverse transcribed into cDNA using oligo (dT) primers (Promega). The resulting cDNA was amplified using MasterMix qPCR SyGreen (PCR Biosystems Ltd). Detection of selected genes was performed on optical-grade 48 well plates in an Eco™ Real-Time PCR System (Illumina).

To analyse the expression of inflammatory mediators in the colons of control, DSS and iMC-treated DSS mice, total colonic RNA was isolated with RNeasy® Mini Kit (Qiagen) using a Precellys 24 homogenizer (Bertin Technologies). Purity and RNA concentration were measured with a NanoDrop™ 2000 spectrophotometer (ThermoFisher Scientific) and reverse transcribed (2 µg/sample) using oligo (dT) primers (Promega). The resulting cDNA was amplified using MasterMix qPCR SyGreen (PCR Biosystems Ltd) in optical-grade 48 well plates, employing an Eco™ Real-Time PCR System (Illumina). The $2^{-\Delta\Delta Ct}$ method was used to normalize expression results. The values of the housekeeping glyceraldehyde-3-phosphate dehydrogenase (*GAPDH*) gene were used to normalize the values obtained for each of the genes. Relative gene expression was calculated by means of $\Delta\Delta Ct$ formula and expressed as fold-change compared with the noncolitic control. Specific primer sequences (Sigma-Aldrich) are presented in Table 1.

## 4.16 | Statistical analysis

Statistical analysis was performed using the GraphPad Prism version 7 software (GraphPad Software, Inc). All data are represented as mean (SEM) of at least 3 independent experiments/biological replicates unless otherwise stated in the figure legends. The Mann-Whitney *U* test for nonparametric data was used for the analysis of the DAI and microscopic score. For the PBMCs proliferation experiment analysis (Figure 2B,C) a two-way ANOVA followed by the Bonferroni post hoc test was performed. For the rest of the data, multiple comparisons between groups were performed using the one-way ANOVA, followed by the Bonferroni post hoc test. A $P < .05$ was considered significant.

## CONFLICT OF INTEREST

The authors declare no conflict of interest.

## DATA AVAILABILITY STATEMENT

The data that support the findings of this study are available from the corresponding authors upon reasonable request.

## ORCID

*Alba Rodríguez-Nogales* https://orcid.org/0000-0003-1927-0628

## REFERENCES

1. Abdel Salam AG, Ata HM, Salman TM, Rashed LA, Sabry D, Schaalan MF. Potential therapeutic utility of mesenchymal stem cells in inflammatory bowel disease in mice. *Int Immunopharmacol*. 2014;22(2):515-521.
2. Kaser A, Zeissig S, Blumberg RS. Inflammatory bowel disease. *Annu Rev Immunol*. 2010;28:573-621.
3. Meirelles LdS, Chagastelles PC, Nardi NB. Mesenchymal stem cells reside in virtually all post-natal organs and tissues. *J Cell Sci*. 2006;119(Pt 11):2204-2213.
4. Owens BM, Simmons A. Intestinal stromal cells in mucosal immunity and homeostasis. *Mucosal Immunol*. 2013;6(2):224-234.
5. Carrillo-Galvez AB, Cobo M, Cuevas-Ocaña S, et al. Mesenchymal stromal cells express GARP/LRRC32 on their surface: effects on their biology and immunomodulatory capacity. *Stem Cells*. 2015;33(1):183-195.
6. de Araújo Farias V, Carrillo-Gálvez AB, Martín F, Anderson P. TGF-β and mesenchymal stromal cells in regenerative medicine, autoimmunity and cancer. *Cytokine Growth Factor Rev*. 2018;43:25-37.
7. Chen X, Zhang ZY, Zhou H, Zhou GW. Characterization of mesenchymal stem cells under the stimulation of Toll-like receptor agonists. *Dev Growth Differ*. 2014;56(3):233-244.
8. Degirmenci B, Valenta T, Dimitrieva S, Hausmann G, Basler K. GLI1-expressing mesenchymal cells from the essential Wnt-secreting niche for colon stem cells. *Nature*. 2018;558(7710):449-453.
9. Nowarski R, Jackson R, Flavell RA. The stromal intervention: regulation of immunity and inflammation at the epithelial-mesenchymal barrier. *Cell*. 2017;168(3):362-375.
10. Beswick EJ, Johnson JR, Saada JI, et al. TLR4 activation enhances the PD-L1-mediated tolerogenic capacity of colonic CD90+ stromal cells. *J Immunol*. 2014;193(5):2218-2229.
11. Thomson CA, Nibbs RJ, McCoy KD, Mowat AM. Immunological roles of intestinal mesenchymal cells. *Immunology*. 2020;160(4):313-324.
12. Scheibe K, Backert I, Wirtz S, et al. IL-36R signalling activates intestinal epithelial cells and fibroblasts and promotes mucosal healing in vivo. *Gut*. 2017;66(5):823-838.
13. Kinchen J, Chen HH, Parikh K, et al. Structural remodeling of the human colonic mesenchyme in inflammatory bowel disease. *Cell*. 2018;175(2):372-386.e317.
14. Huang B, Chen Z, Geng L, et al. Mucosal profiling of pediatric-onset colitis and IBD reveals common pathogenics and therapeutic pathways. *Cell*. 2019;179(5):1160-1176.e1124.
15. Zhao L. The Gut microbiota and obesity: from correlation to causality. *Nat Rev Microbiol*. 2013;11(9):639-647.
16. Krampera M, Pizzolo G, Aprili G, Franchini M. Mesenchymal stem cells for bone, cartilage, tendon and skeletal muscle repair. *Bone*. 2006;39(4):678-683.

17. Krampera M. Mesenchymal stromal cells: more than inhibitory cells. *Leukemia*. 2011;25(4):565-566.

18. Uccelli A, Moretta L, Pistoia V. Immunoregulatory function of mesenchymal stem cells. *Eur J Immunol*. 2006;36(10):2566-2573.

19. Hidalgo-Garcia L, Galvez J, Rodriguez-Cabezas ME, Anderson PO. Can a conversation between mesenchymal stromal cells and macrophages solve the crisis in the inflamed intestine? *Front Pharmacol*. 2018;9:179.

20. Roulis M, Nikolaou C, Kotsaki E, et al. Intestinal myofibroblast-specific Tpl2-Cox-2-PGE2 pathway links innate sensing to epithelial homeostasis. *Proc Natl Acad Sci USA*. 2014;111(43):E4658-E4667.

21. Sacks D, Baxter B, Campbell BCV, et al. Multisociety consensus quality improvement revised consensus statement for endovascular therapy of acute ischemic stroke. *Int J Stroke*. 2018;13(6):612-632.

22. Davis MJ, Tsang TM, Qiu Y, et al. Macrophage M1/M2 polarization dynamically adapts to changes in cytokine microenvironments in *Cryptococcus neoformans* infection. *MBio*. 2013;4(3):e00264-13.

23. Worthley DL, Churchill M, Compton JT, et al. Gremlin 1 identifies a skeletal stem cell with bone, cartilage, and reticular stromal potential. *Cell*. 2015;160(1-2):269-284.

24. Nakanishi C, Nagaya N, Ohnishi S, et al. Gene and protein expression analysis of mesenchymal stem cells derived from rat adipose tissue and bone marrow. *Circ J*. 2011;75(9):2260-2268.

25. Al-Nbaheen M, Vishnubalaji R, Ali D, et al. Human stromal (mesenchymal) stem cells from bone marrow, adipose tissue and skin exhibit differences in molecular phenotype and differentiation potential. *Stem Cell Rev Rep*. 2013;9(1):32-43.

26. Powell DW, Mifflin RC, Valentich JD, et al. Intestinal subepithelial myofibroblasts. *Am J Physiol*. 1999;277(2):C183-C201.

27. Heo JS, Choi Y, Kim HS, Kim HO. Comparison of molecular profiles of human mesenchymal stem cells derived from bone marrow, umbilical cord blood, placenta and adipose tissue. *Int J Mol Med*. 2016;37(1):115-125.

28. Dominici M, Le Blanc K, Mueller I, et al. Minimal criteria for defining multipotent mesenchymal stromal cells. The International Society for Cellular Therapy position statement. *Cytotherapy*. 2006;8(4):315-317.

29. Pinchuk IV, Powell DW. Immunosuppression by intestinal stromal cells. *Adv Exp Med Biol*. 2018;1060:115-129.

30. Pinchuk IV, Beswick EJ, Saada JI, et al. Human colonic myofibroblasts promote expansion of CD4+ CD25high Foxp3+ regulatory T cells. *Gastroenterology*. 2011;140(7):2019-2030.

31. Meisel R, Zibert A, Laryea M, Göbel U, Daubener W, Dilloo D. Human bone marrow stromal cells inhibit allogeneic T-cell responses by indoleamine 2,3-dioxygenase-mediated tryptophan degradation. *Blood*. 2004;103(12):4619-4621.

32. Ciorba MA. Indoleamine 2,3 dioxygenase in intestinal disease. *Curr Opin Gastroenterol*. 2013;29(2):146-152.

33. Galipeau J, Krampera M, Barrett J, et al. International Society for Cellular Therapy perspective on immune functional assays for mesenchymal stromal cells as potency release criterion for advanced phase clinical trials. *Cytotherapy*. 2016;18(2):151-159.

34. West NR, Hegazy AN, Owens BMJ, et al. Oncostatin M drives intestinal inflammation and predicts response to tumor necrosis factor-neutralizing therapy in patients with inflammatory bowel disease. *Nat Med*. 2017;23(5):579-589.

35. Martin JC, Chang C, Boschetti G, et al. Single-cell analysis of Crohn's disease lesions identifies a pathogenic cellular module associated with resistance to anti-TNF therapy. *Cell*. 2019;178(6):1493-1508. e1420.

36. Smillie CS, Biton M, Ordovas-Montanes J, et al. Intra- and intercellular rewiring of the human colon during ulcerative colitis. *Cell*. 2019;178(3):714-730.e722.

37. Caër C, Wick MJ. Human intestinal mononuclear phagocytes in health and inflammatory bowel disease. *Front Immunol*. 2020;11:410.

38. Koelink PJ, Bloemendaal FM, Li B, et al. Anti-TNF therapy in IBD exerts its therapeutic effect through macrophage IL-10 signalling. *Gut*. 2020;69(6):1053-1063.

39. Németh K, Leelahavanichkul A, Yuen PS, et al. Bone marrow stromal cells attenuate sepsis via prostaglandin E(2)-dependent reprogramming of host macrophages to increase their interleukin-10 production. *Nat Med*. 2009;15(1):42-49.

40. Anderson P, Souza-Moreira L, Morell M, et al. Adipose-derived mesenchymal stromal cells induce immunomodulatory macrophages which protect from experimental colitis and sepsis. *Gut*. 2013;62(8):1131-1141.

41. Yang WS, Park BW, Jung EH, et al. Iodide management in formamidinium-lead-halide-based perovskite layers for efficient solar cells. *Science*. 2017;356(6345):1376-1379.

42. Chanput W, Mes JJ, Wichers HJ. THP-1 cell line: an in vitro cell model for immune modulation approach. *Int Immunopharmacol*. 2014;23(1):37-45.

43. Daigneault M, Preston JA, Marriott HM, Whyte MK, Dockrell DH. The identification of markers of macrophage differentiation in PMA-stimulated THP-1 cells and monocyte-derived macrophages. *PLoS One*. 2010;5(1):e8668.

44. Chassaing B, Aitken JD, Malleshappa M, Vijay-Kumar M. Dextran sulfate sodium (DSS)-induced colitis in mice. *Curr Protoc Immunol*. 2014;104(1):11-15.

45. Castelo-Branco MT, Soares ID, Lopes DV, et al. Intraperitoneal but not intravenous cryopreserved mesenchymal stromal cells home to the inflamed colon and ameliorate experimental colitis. *PLoS One*. 2012;7(3):e33360.

46. Wang M, Liang C, Hu H, et al. Intraperitoneal injection (IP), Intravenous injection (IV) or anal injection (AI)? Best way for mesenchymal stem cells transplantation for colitis. *Sci Rep*. 2016;6:30696.

47. Sala E, Genua M, Petti L, et al. Mesenchymal stem cells reduce colitis in mice via release of TSG6, independently of their localization to the intestine. *Gastroenterology*. 2015;149(1):163-176.e120.

48. Stzepourginski I, Nigro G, Jacob JM, et al. CD34+ mesenchymal cells are a major component of the intestinal stem cells niche at homeostasis and after injury. *Proc Natl Acad Sci USA*. 2017;114(4):E506-E513.

49. Karpus ON, Westendorp BF, Vermeulen JLM, et al. Colonic CD90+ crypt fibroblasts secrete semaphorins to support epithelial growth. *Cell Rep*. 2019;26(13):3698-3708.e3695.

50. Brown SL, Riehl TE, Walker MR, et al. Myd88-dependent positioning of Ptgs2-expressing stromal cells maintains colonic epithelial proliferation during injury. *J Clin Investig*. 2007;117(1):258-269.

51. Goessling W, North TE, Loewer S, et al. Genetic interaction of PGE2 and Wnt signaling regulates developmental specification of stem cells and regeneration. *Cell*. 2009;136(6):1136-1147.

52. Soontararak S, Chow L, Johnson V, et al. Mesenchymal Stem Cells (MSC) Derived from Induced Pluripotent Stem Cells (iPSC) equivalent to adipose-derived msc in promoting intestinal healing and microbiome normalization in mouse inflammatory bowel disease model. *Stem Cells Transl Med*. 2018;7(6):456-467.

53. Seno H, Miyoshi H, Brown SL, Geske MJ, Colonna M, Stappenbeck TS. Efficient colonic mucosal wound repair requires Trem2 signaling. *Proc Natl Acad Sci USA*. 2009;106(1):256-261.

54. Owen KA, Abshire MY, Tilghman RW, Casanova JE, Bouton AH. FAK regulates intestinal epithelial cell survival and proliferation during mucosal wound healing. *PLoS One*. 2011;6(8):e23123.

55. Dutra RC, Claudino RF, Bento AF, et al. Preventive and therapeutic euphol treatment attenuates experimental colitis in mice. *PLoS One*. 2011;6(11):e27122.

56. Schmitt M, Schewe M, Sacchetti A, et al. Paneth cells respond to inflammation and contribute to tissue regeneration by acquiring stem-like features through SCF/c-Kit signaling. *Cell Rep*. 2018;24(9):2312-2328.e2317.

57. Plumas J, Chaperot L, Richard MJ, Molens JP, Bensa JC, Favrot MC. Mesenchymal stem cells induce apoptosis of activated T cells. *Leukemia*. 2005;19(9):1597-1604.

58. Akiyama K, Chen C, Wang D, et al. Mesenchymal-stem-cell-induced immunoregulation involves FAS-ligand-/FAS-mediated T cell apoptosis. *Cell Stem Cell*. 2012;10(5):544-555.

59. Gonçalves Fda C, Schneider N, Pinto FO, et al. Intravenous vs intraperitoneal mesenchymal stem cells administration: what is the best route for treating experimental colitis? *World J Gastroenterol*. 2014;20(48):18228-18239.

60. Gonçalves FDC, Luk F, Korevaar SS, et al. Membrane particles generated from mesenchymal stromal cells modulate immune responses by selective targeting of pro-inflammatory monocytes. *Sci Rep*. 2017;7(1):12100.

61. Vega-Letter AM, Kurte M, Fernández-O'Ryan C, et al. Differential TLR activation of murine mesenchymal stem cells generates distinct immunomodulatory effects in EAE. *Stem Cell Res Ther*. 2016;7(1):150.

62. Waterman RS, Tomchuck SL, Henkle SL, Betancourt AM. A new mesenchymal stem cell (MSC) paradigm: polarization into a pro-inflammatory MSC1 or an Immunosuppressive MSC2 phenotype. *PLoS One*. 2010;5(4):e10088.

63. Persson PB. Good publication practice in physiology. *Acta Physiol*. 2019;227(4):e13405.

64. Camuesco D, Rodríguez-Cabezas ME, Garrido-Mesa N, et al. The intestinal anti-inflammatory effect of dersalazine sodium is related to a down-regulation in IL-17 production in experimental models of rodent colitis. *Br J Pharmacol*. 2012;165(3):729-740.

65. Vezza T, Algieri F, Rodriguez-Nogales A, et al. Immunomodulatory properties of *Olea europaea* leaf extract in intestinal inflammation. *Mol Nutr Food Res*. 2017;61(10):1–22.

66. Rodriguez-Nogales A, Algieri F, Vezza T, et al. Calcium pyruvate exerts beneficial effects in an experimental model of irritable bowel disease induced by DCA in rats. *Nutrients*. 2019;11(1):140.